Article

Synthetic Na^+/K^+ exchangers promote apoptosis by disturbing cellular cation homeostasis

Sang-Hyun Park[1,8], Inhong Hwang[2,8], Daniel A. McNaughton,[3,8] Airlie J. Kinross,[3] Ethan N. W. Howe [3,6], Qing He[4,*], Shenglun Xiong[4], Martin Drøhse Kilde[2,7], Vincent M. Lynch[2], Philip A. Gale[3,5*], Jonathan L. Sessler[2,9,*], and Injae Shin[1,*]

[1]Department of Chemistry, Yonsei University, 03722 Seoul, Republic of Korea.
[2]Department of Chemistry, The University of Texas at Austin, 105 East 24th Street, Stop A5300, Austin, Texas 78712, USA.
[3]School of Chemistry (F11), The University of Sydney, Sydney, NSW 2006, Australia.
[4]State Key Laboratory of Chemo/Biosensing and Chemometrics, College of Chemistry and Chemical Engineering, Hunan University, Changsha 410082, P. R. China.
[5]The University of Sydney Nano Institute (SydneyNano), The University of Sydney, Sydney, NSW 2006, Australia
[6]Current address: GlaxoSmithKline, GSK Jurong, 1 Pioneer Sector 1, Singapore 628413
[7]Current address: Department of Chemistry, University of Copenhagen, Universitetsparken 5, DK-2100 Copenhagen Ø, Denmark
[8]These authors contributed equally
[9]Lead Contact
*Correspondence:
heqing85@hnu.edu.cn
philip.gale@sydney.edu.au
sessler@cm.utexas.edu
injae@yonsei.ac.kr

SUMMARY

A number of artificial cation ionophores (or transporters) have been developed for basic research and biomedical applications. However, their mechanisms of action and the putative correlations between changes in intracellular cation concentrations and induced cell death remain poorly understood. Here we show that three hemispherand-strapped calix[4]pyrrole based ion pair receptors act as efficient Na^+/K^+ exchangers in the presence of Cl^- in liposomal models, and promote Na^+ influx and K^+ efflux (Na^+/K^+ exchange) in cancer cells to induce apoptosis. Mechanistic studies reveal that these cation exchangers induce endoplasmic reticulum (ER) stress in cancer cells by perturbing intracellular cation homeostasis, promote generation of reactive oxygen species, and eventually enhance mitochondria-mediated apoptosis. However, they neither induce osmotic stress nor affect autophagy. The present study provides support for the notion that synthetic receptors which perturb cellular cation homeostasis may provide a new approach to generating agents with potentially useful apoptotic activity.

KEYWORDS: Ion pair, Transporter, Calix[4]pyrrole, Receptor, Na^+ influx, K^+ efflux, Reactive oxygen species, Autophagy, Cation homeostasis

INTRODUCTION

The precise regulation of intracellular ion concentrations is essential for diverse cellular functions and eventually sustaining living organisms. A variety of natural ion transporters/channels are responsible for maintaining concentration gradients of ions across cell membranes Recently, several synthetic anion transporters have been developed and their biological activities in cells have been determined.[1] Additionally,

various types of small molecule-based cation carriers or pore-forming molecules have been explored for basic research and biomedical applications.[1] For example, polycyclic ether-based natural products,[2] macrocyclic peptides and depsipeptides,[3-7] crown ethers[8] or peptide-crown ether conjugates[9] and cationic cyclodextrins[10] have been shown to perturb intracellular cation concentrations mainly by forming channels and pores. However, their effects on biological systems have not been well elucidated.

Multiple previous studies have shown that disruption of potassium ion homeostasis in cells is closely related to the onset of apoptosis.[11] Agents that disrupt cellular potassium ion homeostasis can thus induce apoptosis.[8] For instance, valinomycin, a naturally occurring K^+-selective ionophore that enhances K^+ efflux, was found to perturb potassium homeostasis and induce apoptosis in cells.[12, 13] However, the underlying mechanisms of action leading to apoptosis induction have yet to be fully elucidated.[12, 14] Studies of well-defined synthetic transporters can help address this knowledge gap. Here we report a set of artificial ion pair receptors that act as efficient Na^+/K^+ exchangers in liposomal models. They mediate Na^+ influx and promote K^+ efflux in cancer cells. The resulting K^+/Na^+ cation exchange perturbs cellular cation homeostasis and triggers endoplasmic reticulum (ER) stress-associated apoptotic cell death. To the best of our knowledge, this is the first example of an ion pair receptor that has proven effective at inducing apoptosis. It thus highlights a possible new approach to drug discovery while providing specific tools that can be used to modulate intracellular cation concentrations.

RESULTS AND DISCUSSION

Design, synthesis and ion pair-binding studies of hemispherand-strapped calix[4]pyrroles

The goal of this study was to explore whether synthetic receptors could be used to perturb cellular potassium cation homeostasis and the effect, if any, such perturbations would have on apoptosis. Therefore, in terms of receptor design, what was needed were systems that would promote K^+ egress without inducing a substantial change in membrane potential or inducing appreciable osmotic stress. This goal could be met, we felt, by creating carrier systems that would promote intracellular K^+/Na^+ cation exchange rather than the transmembrane movement of a single cation. In operational terms, we felt this would require the use of ion pair receptors that would promote the charged balanced through-membrane transport of both M^+ and Cl^-, where M^+ is either K^+ or Na^+ depending on the direction of cation flow. We also appreciated that the extracellular sodium concentrations (ca. 145 mM) are much higher than their intracellular concentrations (12 mM), whereas the intracellular potassium concentrations (ca. 150 mM) are much higher than the extracellular concentration (ca. 4 mM).[15] In principle, therefore, ion pair receptors that bind to Na^+ or K^+ in the presence of Cl^- but not its absence, would be expected to bind Na^+ and Cl^- outside of cells, where Na^+ ions are present at high concentrations. This would allow for their transport through the cellular membrane in the form of a neutral ion pair complex. Inside cells, where the K^+ concentration is much higher than the Na^+ concentration, Na^+ would be released in favor of K^+ (Na^+/K^+ exchange). The resulting KCl ion pair complex would then exit from cells. Outside the cells, K^+ would be released and new molar equivalent of Na^+ taken up (K^+/Na^+ exchange). As a consequence, it is expected that the transporters would reduce the intracellular K^+ concentration while increasing that of Na^+.

Compounds **1**-**3** (Figure 1a) contain both triaryl cation recognition subunits and a calix[4]pyrrole anion binding motif. They were thus expected to function as ion pair receptors capable of transporting as ion pairs both NaCl and KCl. Systems **4** and **5** were designed as controls for the cation and anion complexation sites, respectively. Receptor **3** was obtained as described previously,[16] whereas analogues **1** and **2**, along with control compound **4**, were synthesized according to the general method of Lee

et al. (Schemes S1 and S2).[17, 18] All new compounds were characterized by standard spectroscopic means. Receptors **1** and **2** were also characterized by means of single crystal X-ray diffraction analysis (Figures S1 and S2).

Initial support for the design expectation that the new receptors **1** and **2** would be able to bind NaCl and KCl as ion pairs came from ^{1}H NMR spectroscopic analysis carried out in CD_2Cl_2. In earlier work, we showed that receptor **3** was capable of binding NaCl and KCl in nitrobenzene-d_5[16]. The same proved true for ion pair receptors **1** and **2**. These latter systems were also found capable of extracting NaCl and KCl from the solid state into CD_2Cl_2 (Figures S3 and S4). Specifically, upon contacting CD_2Cl_2 solutions of **1** or **2** with solid NaCl or KCl and allowing to equilibrate for 48 h, the NH protons of the calix[4]pyrrole moieties of **1** and **2** underwent downfield shifts while the calix[4]pyrrole CH protons shifted upfield. Concurrently, the aromatic proton and the OMe or OCH_2CH_2OMe signals shifted to lower field. These findings are consistent with the chloride anions being bound to the calix[4]pyrrole subunit and the Na^+ or K^+ cations being complexed by the hemispherand straps present in **1** and **2**. In contrast, no appreciable changes in the ^{1}H NMR spectra of **4** and **5** were seen upon exposure to NaCl or KCl under otherwise identical conditions (Figures S5 and S6). Single-crystal X-ray diffraction analyses revealed that both NaCl and KCl are bound as tight ion pairs in the solid state (Figure 1b and Figures S7-S10). As expected, the Na^+ and K^+ cations interact with the hemispherand-amide based straps, while the chloride anions were found bound to cone-shaped calix[4]pyrrole moieties via multiple hydrogen bonding interactions. These structural features mirror what was seen previously in the case of receptor **3**.[16]

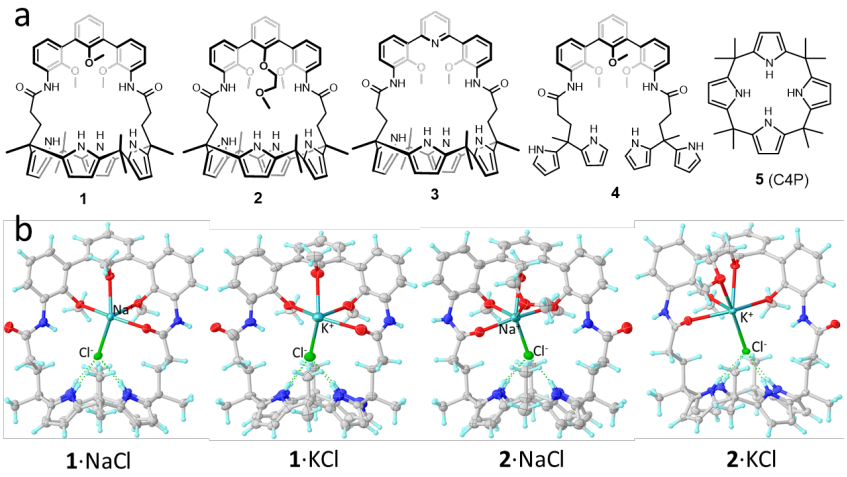

Figure 1. Artificial ion-pair receptors considered in this study.
(a) Chemical structures of compounds 1-5. (b) Partial view of the single-crystal structures of (from left to right) 1·NaCl, 1·KCl, 2·NaCl, and 2·KCl. Solvent molecules are omitted for clarity.

To test the solution phase binding interactions between NaCl or KCl and receptors **1**-**3**, ^{1}H NMR spectroscopic titrations were carried out in a mixture of THF-d_8/D_2O (9 : 1, v/v), a medium selected after considering the solubilities of all species involved. Upon titration with NaCl, receptors **1** appears to bind NaCl with an exchange rate that is intermediate on the NMR time scale, whereas slow and fast exchange are seen in the case of receptors **2** and **3**, respectively (Figures S11-S14). Similar effects were seen in the case of KCl (Figures S15-S19). In contrast, the interactions between receptors (**1**-**3**) and Na^+ (or K^+) were found to be almost negligible (Figures S20-S25). On this basis, we conclude qualitatively that the binding affinities of **1**-**3** for the ion pairs NaCl and KCl follow the order **2** > **1** > **3** and **2** > **1** ≈ **3**, respectively. These conclusions were supported by DFT calculations (Figures S26-S31 and Tables S1 and S2).

Ion-transport activity of strapped calix[4]pyrroles in a liposome model

A series of transport experiments were conducted to determine whether the receptors were capable of facilitating Na^+/K^+ exchange across lipid bilayer membranes. This type of model system has been used extensively to investigate the activity of synthetic chloride transporters. [19-22] In the present instance, a 300 mM KCl solution was encapsulated within the vesicles which were subsequently suspended in a buffered extracellular solution of 300 mM NaCl. A potassium ion-selective electrode was employed to measure the efflux of K^+ ions into the extravesicular solution upon the addition of each putative transporter (see the Supplementary Information for a full description of conditions and methods).

Table 1. Summary of Na^+/K^+ Transmembrane Transport Results of Transporters Used in This Study

	$EC_{50,\ 1800s}$[a]	n[b]	K^+/Na^+ (%s^{-1}) with Cl^-	K^+/Na^+ (%s^{-1})	F_{en}[e]
1	0.39 ± 0.03	1.70 ± 0.02	1.75[c]	0.023[d]	76
2	1.05 ± 0.02	1.90 ± 0.02	0.046[d]	0.031[d]	1.5
3	0.86 ± 0.01	1.70 ± 0.04	0.086[d]	0.034[d]	2.6
4	5.75 ± 0.08	4.00 ± 0.53	0.021[d]	0.018[d]	1.2

a) Concentration of receptor (mol% receptor to lipid) required to achieve 50% potassium efflux at 1800 s during the Na^+/K^+ exchange experiment, using NaCl and KCl as the medium. b) Hill coefficient for the Na^+/K^+ experiment. c) Maximum rate (at 5 mol% receptor to lipid) calculated by fitting the efflux plot to an exponential decay curve using Origin 2019. d) Maximum rate (at 5 mol% receptor to lipid) calculated by fitting the efflux plot to a Boltzmann sigmoidal curve in Origin 2019. e) The ratio of maximum rates; this value was calculated *via* division of the maximum rate in the NaCl/KCl exchange assay by the maximum rate achieved in the corresponding NaGlu/KGlu exchange assay.

Compounds **1**-**3** were all found to facilitate K^+/Na^+ exchange across the lipid bilayer under these experimental conditions. A percentage K^+ efflux at 1800 s was established for each transporter at multiple concentrations and this data was fitted to the Hill equation to determine $EC_{50,1800s}$ values for each transporter. Compound **1** was found to be the most active compound, with an $EC_{50,\ 1800s}$ value of 0.39 mol% (Figure 2c-d and Table 1; see also Figure S32 and Table S3). Compared with **1** and **3**, compound **2** was found to be the least active of the compounds tested (Figures S33 and S34), although the NMR spectral titrations provided evidence that this compound bound the ion pair most strongly. The lower levels of activity may be due to solubility issues, poor partitioning of the transporter into the lipid bilayer, or to the affinity of the ion-pair interaction being too strong to allow decomplexation of the metal cation under the conditions of the transport experiments. A Hill coefficient close to 2 was found in the case of all three compounds; this is consistent with the high Hill coefficients seen previously in the case of transmembrane anion transport experiments involving calixpyrrole derivatives[23, 24] and may reflect the formation of non-1:1 complexes under the conditions of the transport studies.

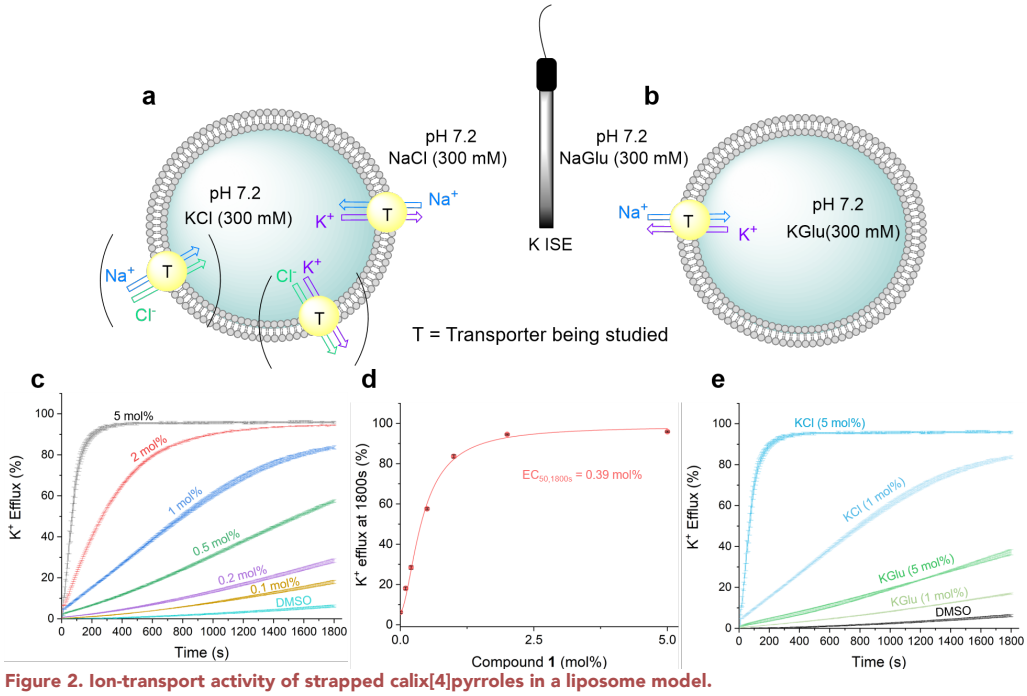

Figure 2. Ion-transport activity of strapped calix[4]pyrroles in a liposome model.
(a) K^+ ISE based assays used in this study to investigate K^+/Na^+ antiport in presence of chloride and (b) absence of chloride. (c) Plots for compound 1 at various concentrations of compound-to-lipid molar ratio. (d) Hill plot analysis for compound 1 of the K^+ efflux at 1800 s against compound-to-lipid molar ratio. Error bars (black) represent the standard deviation of two repeats. (e) Comparison of the K^+/Na^+ antiport plots for compound 1 at two different concentrations of compound-to-lipid molar ratio, running in either KCl/NaCl solutions (blue) or KGlu/NaGlu solutions (green).

Control compound **4** also proved capable of facilitating cation exchange; however, a large Hill coefficient was found, leading us to suggest that several molecules may act cooperatively to bind the ion pair. Moreover, the acyclic system **4** was considerably less active than the macrocyclic calixpyrroles **1**-**3** (Figure S35). In fact, compound **1**, its closest analogue, was almost 15 times more active in the exchange experiments. This difference is rationalized in terms of the additional energetic penalty needed to organize the unconnected pyrrole rings into a chloride binding motif. Compound **5** displayed minimal exchange activity and solubility issues were encountered at higher concentrations. As a consequence, an EC_{50} value could not be determined for this control system. The trend in maximum rate is in accord with the trend in activity, following the sequence **1** > **3** > **2**.

The role of chloride as a coordinating anion was investigated. The above experiments were repeated, this time with 300 mM of potassium gluconate and sodium gluconate as the intracellular and extracellular solutions, respectively (Figure 2b). The gluconate anion does not bind effectively to calixpyrroles. It was thus chosen as a counteranion to investigate whether transporters **1**-**4** would facilitate K^+/Na^+ exchange as cation-only complexes rather than as an ion pair complexes with chloride. All promoted K^+/Na^+ exchange at a slower rate in the absence of chloride than in its presence, indicating importance of Cl^- for K^+/Na^+ exchange (see Supplementary Information for the corresponding efflux plots). The enhanced transport in the presence of chloride was quantified by calculating F_{en}, the ratio of the maximum rate of K^+ efflux in the presence chloride and the maximum rate achieved in the gluconate assay. The difference in rate was most apparent for compound **1** (Figure 2e), where the maximum rate achieved in the chloride assay was 76 times greater; however, compounds **1**-**3** exhibited at least a 50% increase in the maximum rate of cation exchange when chloride was present (Figures S36-40). The presence of chloride presumably increases

the affinity of the receptor towards the respective cations, but also has the effect of neutralizing the charge of the complex. A neutral receptor will be more likely to penetrate the hydrophobic core of the lipid bilayer and traverse the membrane efficiently. Additional transport studies analyzing the M^+/Cl^- symport mechanism and the cation-only M^+/H^+ antiport mechanism of this class of compounds can be found in the Supplementary Information (Figures S41-S56 and Tables S4 and S5).

Ion transport activity of strapped calix[4]pyrroles in cells

In an initial effort to determine whether **1**–**5** could serve as ion transporters in cells, their ability to alter the cellular concentrations of K^+, Na^+, Cl^-, and Ca^{2+} was examined. HeLa and A549 cells were incubated for 2 hours with each compound in the absence and presence of a cellular potassium channel inhibitor, 4-aminopyridine.[25] The levels of cellular potassium ions were then measured using a potassium fluorescent probe PBFI-AM (potassium-binding benzofuran isophthalate acetoxymethyl ester). It was found that incubation with **1**–**3** led to a decrease in the cellular K^+ concentration (Figure 3a and Figure S57a) and that this reduction was not affected by 4-aminopyridine. These findings are consistent with **1**–**3** serving to lower the intracellular K^+ concentrations as a result of artificial receptor-mediated transport rather than through some process involving the cellular potassium channels. In contrast, **4** and **5** without appreciable cation transport activity in liposomes did not affect the intracellular potassium ion levels.

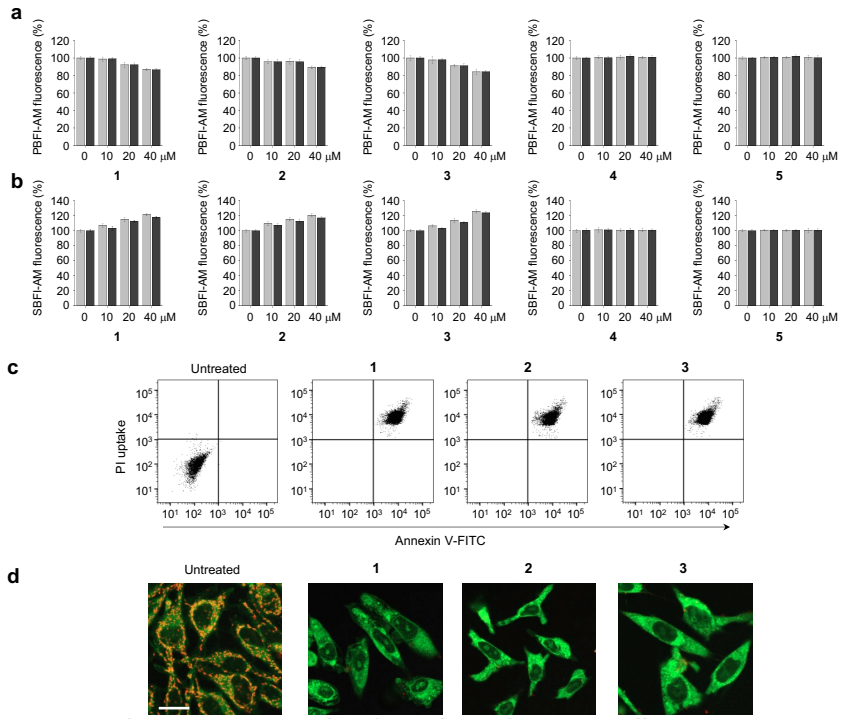

Figure 3. Synthetic transporters with sodium influx and potassium efflux activities promote apoptosis.

(a) HeLa cells pretreated with 10 μM PBFI-AM were incubated with various concentrations of receptors 1-5 in the absence (grey bars) and presence (black bars) of 20 μM 4-aminopyridine for 2 hours. The PBFI fluorescence was used to monitor changes in the intracellular potassium ion concentrations (mean ± s.d., n = 3). (b) HeLa cells pretreated with 10 μM SBFI-AM were incubated for 2 hours with various concentrations of 1-3 in the absence (grey bars) and presence (black bars) of 1 mM amiloride. SBFI-AM fluorescence was used to monitor changes in the intracellular sodium ion concentrations (mean ± s.d., n = 3). (c) Flow cytometry of HeLa cells treated with 20 μM 1, 40 μM 2 or 20 μM 3 for 24 hours and stained with a mixture of fluorescein-annexin V and PI. Untreated cells are shown as a negative control. (d) HeLa cells were treated with 20 μM 1, 40 μM 2 or 20 μM 3 for 24 hours and then stained with JC-1. Cell images of red and green fluorescence

were obtained using confocal fluorescence microscopy at 600 nm and 535 nm, respectively. Shown are merged cell images of the red and green fluorescence (scale bar: 10 μm).

We then examined whether changes in the sodium ion concentrations in cells would be seen after treatment with **1**–**5**. HeLa and A549 cells were thus incubated for 2 hours in the absence and presence of a cellular sodium channel blocker, amiloride,[23, 26, 27] using a sodium fluorescent probe SBFI-AM (sodium-binding benzofuran isophthalate acetoxymethyl ester). Transporters **1**–**3**, but not **4** and **5**, served to increase the cellular Na^+ concentrations (Figure 3b and Figure S57b). The sodium ion transport activities of **1**–**3** were only very slightly changed in the presence of amiloride, leading us to conclude that the increase in the intracellular sodium ion concentration is mediated by **1**–**3**.

Cell studies were also conducted to determine if the present synthetic transporters affected the intracellular Cl^- concentrations. This was done using a chloride ion-sensitive fluorescent quencher MQAE (N-(ethoxycarbonylmethyl)-6-methoxyquinolinium bromide).[28, 29] It was found that the intracellular chloride ion concentrations were only very slightly increased in the presence of **1**–**3** (Figures 57c and S58a). To test further the effect of Cl^- on Na^+ influx and K^+ efflux promoted by **1**–**3**, cells were incubated with each substance, along with **4** and **5**, in normal HEPES buffer or Cl^--free buffer. These studies revealed that whereas **1**–**3** were characterized by good potassium and sodium transport activities in normal HEPES buffer, essentially no cation exchange activity was seen in the Cl^--free medium (Figure S59a and S59b). This finding highlights the fact that Cl^- ions are essential for Na^+ and K^+ transport in the case **1**–**3** and are consistent with the inferences drawn from the initial binding studies, namely that **1**–**3** are effective ion pair receptors.

We also determined the effect of transporters on the calcium ion levels using a calcium fluorescent probe Fluo-4 NW. The results revealed that **1**–**5** had no effect on the cellular calcium ion concentration in cells after a 2-hour incubation period (Figures S57d and S58b). Also, transporters **1-5** did not alter the cytosolic pH, as inferred on the basis of experiments of cells treated with **1**-**5** followed by staining with the pH-sensitive fluorescent probe BCECP (2',7'-bis-(2-carboxyethyl)-5-(and-6)-carboxyfluorescein) (Figure S58c).[26]

Taken together, the findings are consistent with our design expectations, namely that transporters **1**–**3** serve to promote Na^+ influx and K^+ efflux in the presence of normal chloride anion concentrations. Accordingly, we conclude that they thus function primarily as K^+/Na^+ exchangers. Presumably, this exchange is driven initially by the fact that the intracellular K^+ concentration (150 mM) is much higher than that of Na^+ (12 mM).[30]

Cation exchangers induce apoptosis without affecting autophagy

Multiple previous studies have shown that perturbations in intracellular cation homeostasis are closely correlated with the onset of apoptosis.[31-34] On this basis, we sought to determine whether synthetic transporters **1**–**3** or controls **4** and **5** would enhance cell death. We incubated several cancer and normal cell lines (HeLa, cervical cancer cells; A549, lung adenocarcinoma epithelial cells; PLC/PRF/5, liver hepatoma cells; HepG2, liver hepatocellular carcinoma cells; HCT116, colorectal carcinoma cells; MRC-5, lung fibroblast cells; C2C12, myoblast cells; MEF, embryonic fibroblast cells) with various concentrations of each compound for 24 hours. The results of the corresponding MTT (3-(4,5-dimethylthiazol-2-yl)-2,5-diphenyltetrazolium bromide) assays revealed that the number of viable cells after treatment with **1**–**3** decreased in a dose-dependent manner with half maximum inhibitory concentration (IC_{50}) values ranging from 10 to 25 μM, regardless of the cell type (average IC_{50} values; **1**, 19 μM; **2**, 23 μM; **3**, 10 μM) (Figure S60). However, controls **4** and **5** did not affect the cell viability.

We next tested if the cell death promoted by transporters **1**–**3** takes place via apoptosis. Toward this end, HeLa cells were incubated with **1**–**3** and then exposed to

a mixture of fluorescein-annexin V and propidium iodide (PI). Flow cytometry analyses then revealed that the cells treated with **1**–**3** exhibited positive annexin V binding and PI uptake (Figure 3c). This was taken as evidence of apoptosis.[35] Analyses of cell size by flow cytometry revealed that cells treated with **1**–**3** were subject to considerable shrinkage (Figure S61). This finding provides additional support for the proposed apoptosis-inducing activity of **1**–**3**.

Because the loss of mitochondrial membrane potential is a hallmark of apoptosis, this potential was examined using a membrane potential-sensitive JC-1 probe.[36] The results of cell image analyses revealed an increase in green fluorescence arising from JC-1 and a decrease in its red fluorescence in cells treated with **1**–**3**, as would be expected for apoptosis (Figure 3d). Moreover, an increase in DNA fragmentation was also observed in cells treated with **1**–**3** (Figure S62). Collectively, these findings provide further evidence that transporters **1**–**3** have apoptosis-inducing activity.

Because some synthetic ion transporters are known to affect autophagy (a self-eating process)[27], we also examined the affect, if any, compounds **1**–**5** have on this process. In this study, HeLa cells, stably expressing a mRFP-EGFP-LC3 fusion protein (mRFP, monomeric red fluorescence protein; EGFP, enhanced green fluorescence protein), were exposed to **1**–**5**, along with controls torin-1 (an autophagy inducer) and bafilomycin A1 (BfA1, an autophagy inhibitor).[37] Confocal microscopy image analysis of cells treated with **1**–**5** displayed fluorescence patterns similar to those of untreated cells, even though BfA1 shows yellow vesicles arising from merge of GFP and RFP fluorescence, and torin-1 displays red fluorescent vesicles (Figure S63a).[38] Further support for the conclusion that **1**–**5** have no influence on autophagy, came from assessing the levels of LC3-II and p62 cells treated with **1**–**5**. As inferred from western blotting, the levels of LC3-II and p62 were found to be similar to those in untreated cells (Figure S63b). These findings lead us to conclude that compounds **1**–**5** have no effect on autophagy and that transporters **1**–**3** promote cell death by inducing apoptosis without affecting autophagy. The controls **4** and **5** neither induce apoptosis nor affect autophagy.

Cation exchangers promote cell death via ER stress-associated apoptosis

Next, we sought to understand the cellular mechanisms underlying apoptosis induced by ion pair receptors **1**–**3**. Previously, we found that synthetic transporters with the ability to increase cellular ion concentrations induce osmotic stress, an event that leads eventually to apoptosis[23]. We thus tested whether transporters **1**–**3** would induce osmotic stress. Because osmotic stress causes a change in the cell volume,[39] we measured the cell size over a 1.5 hour period using confocal microscopy after incubating HeLa cells with **1**–**3** as well as with a known osmotic stress inducer, sucrose.[40] No appreciable change in cell size was seen for the cells treated with **1**–**3**, whereas sucrose induced an increase in cell size after short-term incubation before recovering back to the original size within 1 hour (Figure S64a).[23]

Further evidence that transporters **1**–**3** are benign in terms of inducing osmotic stress came from studies of p38 phosphorylation in cells treated with **1**–**3** vs. sucrose. Induction of osmotic stress in cells leads to activation of p38 within a short time window[41]. The results of western blot analyses using a phospho-p38 antibody revealed that **1**–**3** did not alter the level of phosphorylated p38; this stands in contrast to sucrose which increased the level of phosphorylated p38 (Figure S64b). Because transporters **1**–**3** mediate Na^+ influx and K^+ efflux, it is likely that, per our design criteria, **1**–**3** do not promote a substantial increase in intracellular ion concentrations and thus do not induce osmotic stress.

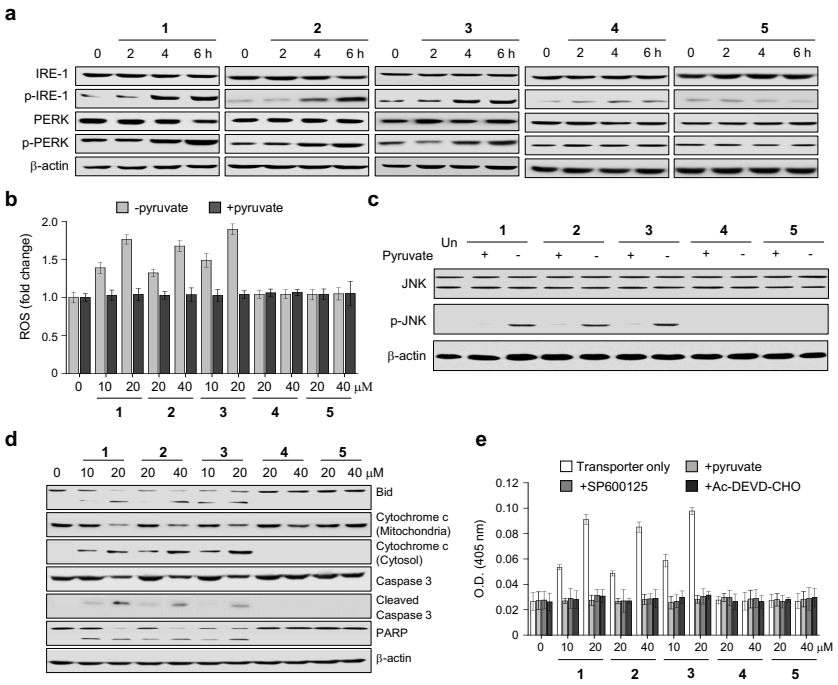

Figure 4. Synthetic ion transporters promote cell death by inducing ER stress.

(a) HeLa cells were treated individually with 20 μM 1, 40 μM 2, 20 μM 3, 40 μM 4 and 40 μM 5 for the indicated times. Immunoblotting was conducted using the indicated antibodies. β-Actin was used as a loading control. (b) HeLa cells were incubated for 8 hours with each substance at indicated concentrations in the presence and absence of 100 mM sodium pyruvate. Treated cells were incubated with 10 μM PF1 for 1 hour. The fluorescence intensity of PF1 was measured using a microplate reader (mean ± s.d., n = 3). (c) HeLa cells were treated individually with 20 μM 1, 40 μM 2 and 20 μM 3, 40 μM 4 and 40 μM 5 for 8 hours. Immunoblotting was conducted using the indicated antibodies. (d) HeLa cells were incubated for 8 hours with each substance at the indicated concentrations for 12 hours. Immunoblotting was conducted using the indicated antibodies. (e) HeLa cells were treated with each substance at the indicated concentrations in the presence and absence of either 100 mM pyruvate or 20 μM SP600125 for 18 hours. The caspase activities of cell lysates were determined using Ac-DEVD-pNA (200 μM) in the absence and presence of 20 μM Ac-DEVD-CHO (mean ± s.d., n = 3).

It has been shown that perturbation of cellular K^+ homeostasis promotes apoptosis by inducing ER stress.[32-34, 42, 43] Accordingly, we examined whether transporters **1**–**3** induce ER stress by determining the levels of phosphorylated IRE-1 and PERK, which are well-known ER stress markers.[44] Immunoblot analysis of HeLa cells incubated with **1**–**5** for various times revealed that the levels of phosphorylated IRE-1 and PERK increased after 4 hours in the case of **1**–**3** but not with **4** and **5** (Figure 4a). These findings are taken as evidence that **1**–**3** induce ER stress in cells.

Because reactive oxygen species (ROS) are produced during ER stress,[45] the ROS levels were determined; this was done by incubating cells with **1**–**5** in the absence and presence of the ROS scavenger sodium pyruvate.[46] Cell studies using the ROS fluorescent probe PF1[46] revealed that the levels of ROS increased in cells treated with **1**–**3** after a 4 hour incubation period but not with **4** and **5** (Figure 4b and Figure S65a). However, when the ROS scavenger was added to the cells treated with **1**–**3**, ROS generation was almost completely eliminated. In addition, it is also known that during ER stress, Ca^{2+} is released from ER into the cytosol.[47] Thus, we determined if the cytosolic Ca^{2+} concentration is changed in cells treated with synthetic transporters using Fluo-4 NW. The results revealed that **1**–**5** had no effect on the cytosolic Ca^{2+} concentration within a 2-hour incubation period (Figures S57d and S65b). However, the cytosolic Ca^{2+} concentration of cells treated with **1**-**3**, but not with **4** and **5**,

increased after a 4 hour incubation period, a time point where the levels of ER stress markers increase and ROS levels become elevated.

An increase in the level of ROS during ER stress is known to induce caspase-dependent apoptosis by activating JNK.[48] To test this, HeLa cells were incubated with **1**–**5** and the level of phosphorylated JNK in the treated cells was then measured by western blotting. Cells treated with **1**–**3** displayed a significant increase in the level of phosphorylated JNK compared to untreated cells (Figure 4c). As expected from the inability of **4** and **5** to generate ROS, they had no effect on the phosphorylation of JNK. To examine further whether ROS generation causes phosphorylation of JNK, HeLa cells were co-treated with **1**–**3** and the ROS scavenger (sodium pyruvate). The phosphorylated form of JNK was then assessed. The results of immunoblot analysis revealed that the ROS scavenger suppressed almost completely the formation of phosphorylated JNK in cells treated with **1**–**3**. This is consistent with the notion that ROS generation promotes JNK activation.

It is known that JNK activation enhances cleavage of Bid and release of cytochrome c from mitochondria into the cytosol for caspase activation.[49] Therefore, HeLa cells treated with **1**–**5** were subjected to western blotting to assess Bid cleavage, as well as the levels of cytosolic and mitochondrial cytochrome c. It was found that Bid was cleaved in cells treated with **1**–**3** and that cytochrome c was released from the mitochondria into the cytosol (Figure 4d). However, **4** and **5** had no effect on these events.

Because cytochrome c is released from mitochondria into the cytosol, we tested whether **1**–**3** would promote caspase activation.[50] Toward this end, the cleavage of procaspase-3 and an endogenous caspase substrate, PARP, was examined. Western blot analyses revealed that the cleaved products of procasepase-3 and PARP were generated in cells treated with **1**–**3**. This was not the case for cells treated with **4** and **5** (Figure 4d). Next, the caspase activities of lysates of cells treated with **1**–**5** were tested using a colorimetric peptide substrate for caspases. It was found that the caspase activity in cells treated with **1**–**3** was increased (Figure 4e). However, when Ac-DEVD-CHO, a known inhibitor of caspases, was added to the lysates of cells treated with **1**–**3**, the caspase activities were attenuated to the basal level. In addition, almost no caspase activity was detected when cells were co-treated with **1**–**3** and either a ROS scavenger (sodium pyruvate) or SP600125 (a selective inhibitor of JNK) (Figure 4e).[51] We thus conclude that the enhanced caspase activity seen in the case of **1**–**3** is induced by ROS generation and JNK activation. Caspase activity was not increased in cells treated with **4** and **5**.

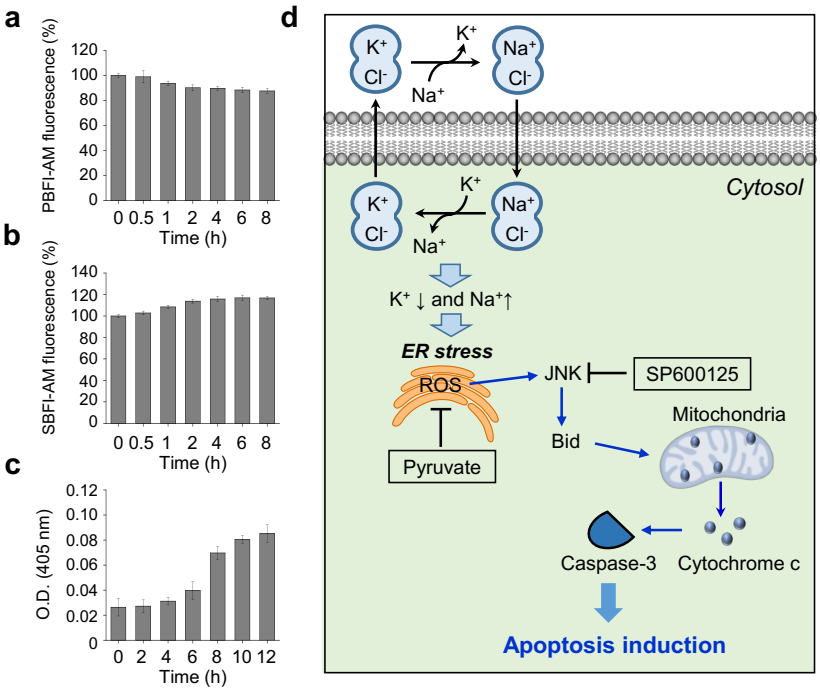

Figure 5. Potassium efflux and sodium influx precede apoptosis induced by a synthetic transporter.

(a) HeLa cells pretreated with 10 μM PBFI-AM were incubated with 20 μM 3 for indicated times. The PBFI fluorescence was measured to examine changes in the intracellular potassium ion concentration (mean ± s.d., n = 3). (b) HeLa cells pretreated with 10 μM SBFI-AM were incubated with 20 μM 3 for the indicated times. SBFI-AM fluorescence was measured to determine changes in the intracellular sodium ion concentration (mean ± s.d., n = 3). (c) HeLa cells were incubated with 20 μM 3 for the indicated times. The caspase activities of cell lysates were determined using Ac-DEVD-pNA (200 μM) (mean ± s.d., n = 3). (d) Proposed mechanism of action underlying the apoptosis induced by the synthetic K^+/Na^+ cation exchangers of this study (see text for a detailed explanation).

Finally, we evaluated whether the change in relative intracellular Na^+ and K^+ cation concentrations promoted by **1**–**3** is a cause or a consequence of caspase-dependent apoptosis. HeLa cells were incubated with each compound at different time periods and then treated with SBFI-AM and PBFI-AM. In addition, the caspase activity of the treated cells was measured in a time-dependent manner. These studies revealed that Na^+ influx and K^+ efflux took place shortly after incubation with **1**–**3** but that increases in caspase activity occurred at later times (Figure 5a-c, Figures S66 and S67). As we also showed, ER stress is seen after incubation of cells with **1**–**3** for ca. 4 hours (Figures 4a and Figure S65). We thus conclude that the perturbations in cellular cation concentrations promoted by **1**–**3** precede ER stress. The disruption of cellular cation homeostasis induced by **1**–**3** leads to ER stress, which is followed by caspase activation. We thus rule out apoptosis leading to the observed changes in cation flux. On the basis of the above mechanistic studies, we propose that ion pair receptors **1**–**3** induce ER stress by perturbing cellular cation homeostasis, enhancing cellular ROS levels, inducing JNK activation and Bid cleavage, promoting the release of cytochrome c from the mitochondria into the cytosol, and inducing caspase activation (Figure 5d). Treatment with either a ROS scavenger or a JNK inhibitor blocks the caspase activation induced by **1**–**3**, as would be expected based on this mechanistic proposal. In addition, transporters **1**-**3** display Na^+/K^+ exchange activity in cells only in the presence of Cl^-. We take this as evidence that Cl^- is required for the cation transport promoted by these receptors. Since transporters **1**-**3** serve as electroneutral ionophores without substantially increasing cellular ion concentrations, they do not induce osmotic stress. Furthermore, **1**–**3** do not affect the autophagy process.

CONCLUSION

We previously demonstrate that synthetic chloride ion transporters induce apoptosis by increasing intracellular chloride and sodium concentrations in cells and consequently provoking osmotic stress.[23] In addition, certain synthetic chloride ion transporters inhibited the autophagic process by disrupting lysosome function through a transporter-mediated decrease in lysosomal chloride ion concentration and an increase in the lysosomal pH.[23,27] Also, it is known that valinomycin, a potassium ionophore, decreases intracellular K^+ concentrations and causes depolarization and uncoupling of respiration in mitochondria by increasing membrane permeability, thereby leading to apoptosis.[14] However, the mode of action whereby valinomycin induces apoptosis has not been fully elucidated. Recently, helical polypeptide-based potassium ionophores were developed that decreased intracellular K^+ concentration and slightly increased the intracellular Ca^{2+} concentration in early times post-treatment without affecting intracellular Na^+ and Cl^- concentrations.[52] It is likely that helical polypeptide-based potassium ionophores act as electrogenic ionophores, similarly to valinomycin. These substances promoted ER stress by disrupting intracellular K^+ concentrations, followed by cytochrome c release and caspase 3 activation.

In the current study we have shown that three synthetic hemispherand-strapped calix[4]pyrroles **1**–**3** act as effective contact ion pair receptors for NaCl and KCl and promote the through-membrane transport of these salts in liposomal models. These synthetic receptors mediate K^+ efflux and Na^+ influx in cells, thus acting effectively as K^+/Na^+ exchangers *in vitro*. Receptors **1**–**3**, but not **4**–**5**, induce apoptosis without affecting autophagy. In addition, **1**–**3** did not induce osmotic stress. Cell studies support the conclusion that receptors **1**–**3** induce ER stress-associated apoptotic cell death by perturbing intracellular cation homeostasis.

Receptors **1**–**3** are different from our previously reported synthetic chloride ion transporters in that they act as Na^+/K^+ exchangers without substantially increasing cellular ion concentrations. In contrast, our previously reported anion transporters serve to increase cellular ion concentrations. Thus, the determinants underlying apoptosis induction differ for these two types of transporters as detailed above. In addition, receptors **1**–**3** differ from valinomycin and helical polypeptide-based potassium ionophores in terms of their mode of transport. Specifically, compounds **1**–**3** act as electroneutral cation exchangers to maintain charge balance during cation transport. However, valinomycin and helical polypeptide-based potassium ionophores serve as electrogenic ionophores. As a consequence, transporters **1**–**3** regulate cellular ion concentrations in a manner distinct from both previous synthetic anion transporters and K^+ ionophores.

Based on the present findings, we suggest that ion pair receptors **1**–**3** could emerge as chemical tools that are useful in modulating intracellular cation concentrations and promoting apoptosis via modes of action that differ from the approaches normally used to trigger programmed cell death. More broadly, synthetic cation exchangers, such as those described here, offer a new approach to generating agents with potentially useful apoptotic activity.

EXPERIMENTAL PROCEDURES

Full experimental procedures are provided in the Supplemental Information.

SUPPLEMENTAL INFORMATION

The Supplemental Information is available free of charge on the website.

Synthesis and characterization of precursors and receptors **1** and **2**; crystallographic details for **1**, **2** and their complexes, NMR data; DFT calculations and other experiment details (PDF)

Crystallographic structure of **1** (CIF), CCDC: 2063566.

Crystallographic structure of **1**·NaCl complex (CIF), CCDC: 2063568.
Crystallographic structure of **1**·KCl complex (CIF), CCDC: 2063569.
Crystallographic structure of **2** (CIF), CCDC: 2063567.
Crystallographic structure of **2**·NaCl complex (CIF), CCDC: 2063570.
Crystallographic structure of **2**·KCl complex (CIF), CCDC: 2063571.

AUTHOR CONTRIBUTIONS

Q.H., P.A.G., J.L.S., and I.S. designed and supervised the project. S-H.P. performed biological studies. Q.H., I-H.W., S.X. and M.D.K. designed and synthesized the compounds and performed ion-binding studies in solution. Q.H. and V.M.L. carried out the X-ray single-crystal structure analysis. Q.H. carried out the DFT calculations. P.A.G., D.A.M, A.J.K. and E.N.W.H, designed and performed the ion-transport studies in liposomes. S-H.P., Q.H. and D.A.M wrote the manuscript. I.S., J.L.S. and P.A.G. helped with writing the manuscript.

ACKNOWLEDGMENTS

The work at Yonsei University was supported financially by the National Research Foundation of Korea (NRF) (grant no. 2020R1A2C3003462 to I.S). The research at Hunan University was funded by the National Natural Science Foundation of China (21901069 and 22071050 to Q. H.), the Science and Technology Plan Project of Hunan Province, China (grant number 2019RS1018 to Q. H.), and Fundamental Research Funds for the Central Universities (Startup Funds to Q. H.). D.A.M., A.J.K., E.N.W.H. and P.A.G. acknowledge and pay respect to the Gadigal people of the Eora Nation, the traditional owners of the land on which we research, teach and collaborate at the University of Sydney. P.A.G. thanks the Australian Research Council (DP200100453) and the University of Sydney for funding, and Xin Wu and LiJun Chen for help with the preparation of this manuscript. The work in Austin was supported initially by the National Institutes of Health (grant R01GM103790 to J.L.S.) with subsequent support provided by the Robert A. Welch Foundation (F-0018 to J.L.S.).

REFERENCES AND NOTES

1. Alfonso, I. & Quesada, R. (2013). Biological activity of synthetic ionophores: ion transporters as prospective drugs? *Chem. Sci. 4*, 3009-3019.
2. Nicolaou, K.C., Frederick, M.O. & Aversa, R.J. (2008). The continuing saga of the marine polyether biotoxins. *Angew. Chem. Int. Ed. 47*, 7182-7225.
3. Gentilucci, L., Tolomelli, A. & Squassabia, F. (2006). Peptides and peptidomimetics in medicine, surgery and biotechnology. *Curr. Med. Chem. 13*, 2449-2466.
4. Sarabia, F., Chammaa, S., Ruiz, A.S., Ortiz, L.M. & Herrera, F.J.L. (2004). Chemistry and biology of cyclic depsipeptides of medicinal and biological interest. *Curr. Med. Chem. 11*, 1309-1332.
5. Ohnishi, M. & Urry, D.W. (1970). Solution Conformation of Valinomycin-Potassium Ion Complex. *Science 168*, 1091-1092.
6. Duax, W.L., Hauptman, H., Weeks, C.M. & Norton, D.A. (1972). Valinomycin Crystal Structure Determination by Direct Methods. *Science 176*, 911-914.
7. Fernandez-Lopez, S. *et al.* (2001). Antibacterial agents based on the cyclic D,L-alpha-peptide architecture. *Nature 412*, 452-455.
8. Kralj, M., Tusek-Bozic, L. & Frkanec, L. (2008). Biomedical Potentials of Crown Ethers: Prospective Antitumor Agents. *ChemMedChem 3*, 1478-1492.
9. Boudreault, P.L. & Voyer, N. (2007). Synthesis, characterization and cytolytic activity of alpha-helical amphiphilic peptide nanostructures containing crown ethers. *Org. Biomol. Chem. 5*, 1459-1465.
10. Yamamura, H. *et al.* (2012). Mimicking an antimicrobial peptide polymyxin B by use of cyclodextrin. *Chem. Commun. 48*, 892-894.

11. Remillard, C.V. & Yuan, J.X.J. (2004). Activation of K+ channels: an essential pathway in programmed cell death. *Am. J. Physiol-Lung C 286*, L49-L67.
12. Abdalah, R., Wei, L., Francis, K. & Yu, S.P. (2006). Valinomycin-induced apoptosis in Chinese hamster ovary cells. *Neurosci. Lett. 405*, 68-73.
13. Klein, B., Worndl, K., Lutz-Meindl, U. & Kerschbaum, H.H. (2011). Perturbation of intracellular K^+ homeostasis with valinomycin promotes cell death by mitochondrial swelling and autophagic processes. *Apoptosis 16*, 1101-1117.
14. Inai, Y. *et al.* (1997). Valinomycin Induces Apoptosis of Ascites Hepatoma Cells (AH-130) in Relation to Mitochondrial Membrane Potential. *Cell Struct. Funct. 22*, 555-563.
15. Yu, S.P., Canzoniero, L.M.T. & Choi, D.W. (2001). Ion homeostasis and apoptosis. *Curr. Opin. Cell Biol. 13*, 405-411.
16. He, Q. *et al.* (2018). Selective Solid-Liquid and Liquid-Liquid Extraction of Lithium Chloride Using Strapped Calix[4]pyrroles. *Angew. Chem. Int. Ed. 57*, 11924-11928.
17. Yoon, D.W., Hwang, H. & Lee, C.H. (2002). Synthesis of a strapped calix[4]pyrrole: Structure and anion binding properties. *Angew. Chem. Int. Ed. 41*, 1757-1759.
18. Lee, C.H., Miyaji, H., Yoon, D.W. & Sessler, J.L. (2008). Strapped and other topographically nonplanar calixpyrrole analogues. Improved anion receptors. *Chem. Commun.*, 24-34.
19. Wu, X. *et al.* (2016). Nonprotonophoric Electrogenic Cl- Transport Mediated by Valinomycin-like Carriers. *Chem 1*, 127-146.
20. Gilchrist, A.M. *et al.* (2020). Tetrapodal Anion Transporters. *Molecules 25*, 5179.
21. Picci, G. *et al.* (2020). Simple isophthalamides/dipicolineamides as active transmembrane anion transporters. *Supramol. Chem. 32*, 112-118.
22. Jowett, L.A. & Gale, P.A. (2019). Supramolecular methods: the chloride/nitrate transmembrane exchange assay. *Supramol. Chem. 31*, 297-312.
23. Park, S.H. *et al.* (2019). Determinants of Ion-Transporter Cancer Cell Death. *Chem 5*, 2079-2098.
24. Clarke, H.J., Wu, X., Light, M.E. & Gale, P.A. (2020). Selective anion transport mediated by strap-extended calixpyrroles. *J. Porphyr. Phthalocya. 24*, 473-479.
25. Choquet, D. & Korn, H. (1992). Mechanism of 4-aminopyridine action on voltage-gated potassium channels in lymphocytes. *J. Gen. Physiol. 99*, 217-240.
26. Ko, S.K. *et al.* (2014). Synthetic ion transporters can induce apoptosis by facilitating chloride anion transport into cells. *Nat. Chem. 6*, 885-892.
27. Busschaert, N. *et al.* (2017). A synthetic ion transporter that disrupts autophagy and induces apoptosis by perturbing cellular chloride concentrations. *Nat. Chem. 9*, 667-675.
28. Cho, H.J. *et al.* (2011). A Small Molecule That Binds to an ATPase Domain of Hsc70 Promotes Membrane Trafficking of Mutant Cystic Fibrosis Transmembrane Conductance Regulator. *J. Am. Chem. Soc. 133*, 20267-20276.
29. Park, S.H., Hyun, J.Y. & Shin, I. (2019). A lysosomal chloride ion-selective fluorescent probe for biological applications. *Chem. Sci. 10*, 56-66.
30. Stauber, T. & Jentsch, T.J. (2013). Chloride in Vesicular Trafficking and Function. *Annu. Rev. Physiol. 75*, 453-477.
31. Bortner, C.D. & Cidlowski, J.A. (2014). Ion channels and apoptosis in cancer. *Philos. T. R. Soc. B 369*, 20130104.
32. Cain, K., Langlais, C., Sun, X.M., Brown, D.G. & Cohen, G.M. (2001). Physiological concentrations of K^+ inhibit cytochrome c-dependent formation of the apoptosome. *J. Biol. Chem. 276*, 41985-41990.
33. Hughes Jr, F.M., Bortner, C.D., Purdy, G.D. & Cidlowski, J.A. (1997). Intracellular K^+ Suppresses the Activation of Apoptosis in Lymphocytes. *J. Biol. Chem. 272*, 30567-30576.

34. Yu, S.P. (2003). Regulation and critical role of potassium homeostasis in apoptosis. *Prog. Neurobiol. 70*, 363-386.
35. Williams, D.R., Ko, S.K., Park, S., Lee, M.R. & Shin, I. (2008). An apoptosis-inducing small molecule that binds to heat shock protein 70. *Angew. Chem. Int. Ed. 47*, 7466-7469.
36. Salvioli, S., Ardizzoni, A., Franceschi, C. & Cossarizza, A. (1997). JC-1, but not DiOC6(3) or rhodamine 123, is a reliable fluorescent probe to assess $\Delta\Psi$ changes in intact cells: implications for studies on mitochondrial functionality during apoptosis. *FEBS Letters 411*, 77-82.
37. Baek, K.H., Park, J. & Shin, I. (2012). Autophagy-regulating small molecules and their therapeutic applications. *Chem. Soc. Rev. 41*, 3245-3263.
38. Park, S.H., Baek, K.H., Shin, I. & Shin, I. (2018). Subcellular Hsp70 Inhibitors Promote Cancer Cell Death via Different Mechanisms. *Cell Chem. Biol. 25*, 1242-1254.
39. Sachs, F. & Sivaselvan, M.V. (2015). Cell volume control in three dimensions: Water movement without solute movement. *J. Gen. Physiol. 145*, 373-380.
40. Andronic, J. *et al.* (2015). Hypotonic Activation of the Myo-Inositol Transporter SLC5A3 in HEK293 Cells Probed by Cell Volumetry, Confocal and Super-Resolution Microscopy. *Plos One 10,* e0119990.
41. Zhou, X.Y., Naguro, I., Ichijo, H. & Watanabe, K. (2016). Mitogen-activated protein kinases as key players in osmotic stress signaling. *BBA-Gen. Subjects 1860*, 2037-2052.
42. Zeeshan, H.M.A., Lee, G.H., Kim, H.R. & Chae, H.J. (2016). Endoplasmic Reticulum Stress and Associated ROS. *Int. J. Mol. Sci. 17*, 327.
43. Thompson, G.J., Langlais, C., Cain, K., Conley, E.C. & Cohen, G.M. (2001). Elevated extracellular [K^+] inhibits death-receptor- and chemical-mediated apoptosis prior to caspase activation and cytochrome c release. *Biochem. J. 357*, 137-145.
44. Oslowski, C.M. & Urano, F. (2011). Measuring Er Stress and the Unfolded Protein Response Using Mammalian Tissue Culture System. *Method. Enzymol. 490*, 71-92.
45. Cao, S.S. & Kaufman, R.J. (2014). Endoplasmic Reticulum Stress and Oxidative Stress in Cell Fate Decision and Human Disease. *Antioxid. Redox Sign. 21*, 396-413.
46. Pai, J. *et al.* (2016). Carbohydrate microarrays for screening functional glycans. *Chem. Sci. 7*, 2084-2093.
47. Deniaud, A. *et al.* (2008). Endoplasmid reticulum stress induces calcium-dependent permeability transition, mitochondrial outer membrane permeabilization and apoptosis. *Oncogene 27*, 285-299.
48. Shen, H.M. & Liu, Z.G. (2006). JNK signaling pathway is a key modulator in cell death mediated by reactive oxygen and nitrogen species. *Free Radical Bio. Med. 40*, 928-939.
49. Dhanasekaran, D.N. & Reddy, E.P. (2008). JNK signaling in apoptosis. *Oncogene 27*, 6245-6251.
50. Li, P. *et al.* (1997). Cytochrome c and dATP-Dependent Formation of Apaf-1/Caspase-9 Complex Initiates an Apoptotic Protease Cascade. *Cell 91*, 479-489.
51. Bennett, B.L. *et al.* (2001). SP600125, an anthrapyrazolone inhibitor of Jun N-terminal kinase. *Proc. Natl. Acad. Sci. USA 98*, 13681-13686.
52. Lee, D. et al. (2019). A Helical Polypeptide-Based Potassium Ionophore Induces Endoplasmic Reticulum Stress-Mediated Apoptosis by Perturbing Ion Homeostasis. *Adv. Sci.* 6, 1801995.